



One-point calibration and matrix-matching concept for quantification of potentially toxic elements in wood by LA-ICP-MS

Danielle da Silva Francischini^{1,2} · Marco Aurélio Zezzi Arruda^{1,2}

Received: 12 August 2023 / Revised: 25 September 2023 / Accepted: 11 October 2023 / Published online: 4 November 2023
© The Author(s), under exclusive licence to Springer-Verlag GmbH, DE part of Springer Nature 2023

Abstract

The aim of this work is to evaluate two quantitative methods, based on the external calibration applied in laser ablation inductively coupled plasma mass spectrometry (LA-ICP-MS) analysis, known as (i) analytical curve and (ii) one-point calibration, using the concept of matrix matching to quantify three potentially toxic elements (PTEs) in wood samples. These can biologically register changes in the abiotic environment and be applied to monitoring climate change or environmental toxicity. In this case, standard sample preparation was evaluated to prepare the standard pellets using *Pinus taeda* species as a matrix-matching concept. Six pellets of *P. taeda*, with different Pb, Cd, and Ba concentrations, were prepared to build the analytical curve and one-point calibration strategies. The LA-ICP-MS parameters were optimised for ²⁰⁶Pb, ²⁰⁸Pb, ¹¹²Cd, ¹¹⁴Cd, ¹³⁷Ba, and ¹³⁸Ba isotope analysis in wood samples. The two calibration strategies provided 74–110% analytical recovery from certified reference materials and similar results to those obtained by ICP-MS through the acid digestion of environmental wood samples from São Paulo City (Brazil). This demonstrated the applicability of the one-point calibration strategy in quantifying PTEs in wood samples, which could be used with environmental analyses. Differences observed between the Ba isotope results obtained via LA-ICP-MS and ICP-MS quantification were related to sampling by LA-ICP-MS and the ICP-MS sample introduction, as well as to laser matrix and transport effects because of the difference between the wood species evaluated.

Keywords Matrix-matching · One-point · Analytical curve · Quantitative analysis · LA-ICP-MS · Wood

Introduction

Dendrochemistry (dendroanalysis) is an area of science devoted to evaluating the variability in essential and non-essential chemical components in wood samples. Wood can biologically register annual changes in the abiotic environment by the growing rings (known as tree rings), allowing the chronological study of climate and environmental

changes [1]. In this context, these samples can be used as proxies for monitoring climate change or environmental toxicity because they can incorporate elements present in the air and soil [1, 2].

Sources of chemical compounds in the environment can be related to natural events, such as changes in pH, water precipitation, and temperature, as well as anthropogenic actions, such as automotive fuel and industrial wastes. Both contribute to the availability of elements in the soil and, consequently, in wood samples [2–4]. Therefore, elemental quantification in this type of sample allows the true environmental impact in terms of concentration to be assessed.

There are 104 chemical elements in the periodic table, some of which are known to be potentially toxic elements (PTEs), such as Pb, Cd, and Ba, that require attention in environmental analysis and are chemicals frequently assessed during water quality analysis in São Paulo (Brazil) [5]. PTEs are metals that are naturally present in the environment but, depending on their concentrations, can present toxic effects instead of benefits or nutrition to the

Published in the topical collection *Elemental Mass Spectrometry for Bioanalysis* with guest editors Jörg Bettmer, Mario Cortez-Rodríguez, and Márcia Foster Mesko.

✉ Marco Aurélio Zezzi Arruda
zezzi@unicamp.br

¹ Spectrometry, Sample Preparation and Mechanization Group (GEPAM), Institute of Chemistry, University of Campinas, PO Box 6154, Campinas, SP 13083-970, Brazil

² National Institute of Science and Technology for Bioanalytics, Institute of Chemistry, University of Campinas, Campinas, SP, Brazil

environment or biological organisms [6, 7]. Lead is one of the most common contaminants in the environment because of industrial effluents and car fuel [8, 9], whilst cadmium is derived from industrial wastes, mining, and phosphate fertilisers [10], and barium is related to pesticide wastes, mining, coal, diesel combustion, and waste incineration [11]. Thus, the real concentration of these PTEs in wood samples can be used for the evaluation of environmental pollution.

Among the different techniques for elemental determination, laser ablation–inductively coupled plasma–mass spectrometry (LA-ICP-MS) presents advantageous applications in solid sample analysis and has been shown to enable analysis of major and minor chemical elements using high LA resolution, high sensitivity, and low background signal [12]. Briefly, this technique consists of the application of a UV laser pulse to a sample surface by lines or spots of ablation. Evaporation of a small portion of the sample forms a dry aerosol, in which all chemical elements present in the aerosol are transported into the ICP-MS, where they are atomised and ionised by plasma at high temperatures. Each chemical element is then analysed by a mass analyser, according to each ion mass-to-charge ratio (m/z) [13]. In the literature, different LA-ICP-MS applications have been described over the years in biomedical research [14], such as single-cell imaging to evaluate breast cancer cells [15], environmental analysis for observing nanoparticle distribution from particulate matter air exposure [16], and quantitative elemental distribution in rock samples [17].

The selection of a suitable calibration method is one of the major difficulties in achieving total quantitative analysis by LA-ICP-MS, due to the matrix and mass fractionation effects caused by laser–sample interaction and transport to the ICP-MS, as well as the lack of certified reference material (CRM) for the preparation of calibration samples and the analytical validation steps [18, 19]. The main sources of error in quantitative analysis by LA-ICP-MS were presented in Limbeck et al. (2015), who evaluated each step of the process, including laser parameters and sample composition, particle size, and aerosol transport, as well as the incomplete ionisation of chemical elements [20]. An adequate calibration strategy for each sample type and/or application must be carefully evaluated and optimised.

Different calibration strategies developed to minimise adverse effects on LA-ICP-MS are reported in the literature. These include external calibration, the matrix-matching concept, internal standards, and the use of liquid standard solutions [21, 22]. Matrix-matching calibration consists of using the matrix itself, a similar matrix, or a certified reference material (CRM) to perform the evaluation of instrumental parameters and to prepare the analytical points used in the external calibration by analytical curves. This makes the sample–laser interactions, both in the matrix of interest and

in the analytical points, similar for avoiding matrix effects [19, 23, 24].

The quantification methods correlate the concentration of the analyte with the analytical response obtained through instrumental analysis. In LA-ICP-MS, the application of linear analytical curves can be considered in order to obtain the elemental concentration, for example as proposed by Pessôa et al. (2017) for quantifying the translocation and accumulation of metals in sunflower seeds using the matrix-matching concept to build the analytical curve [22]. Moreau and Arruda (2022) used filter paper as a solid support for the direct calibration of Cu and Zn in tree ring samples [25]. Hirata et al. (2016) obtained quantitative multi-elemental images of ferromanganese nodules from Japan by applying a calibration curve using developed calibration standards, which could thus provide information about future paleoenvironmental changes [26].

However, for obtaining the analytical curves in LA-ICP-MS, the more points there are on the calibration curve, the more space in the ablation chamber is needed. Additionally, this process is time-consuming, requiring long analysis time and high costs.

As a way to address this issue, the external calibration known as one-point (or single-point), reported by Jochum et al. (2007), uses only one analytical point with a known concentration of the chemical elements, which can be obtained from a CRM pellet or through a matrix-matching approach. When considering one-point calibration, this point is used to calculate the final concentration of the analytes in the sample through mathematical equations [27]. In the literature, it is possible to observe methods that use one, two, or more analytical points for elemental quantification for laser-induced breakdown spectroscopy (LIBS), as presented in the recent review by Costa et al. (2020) [21], a technique that also uses laser ablation for element excitation, but detection is done through the energy emission of the ionised elements in the plasma.

The one-point method proposed shows advantages for application in total quantitative analysis. The advantages include minimisation of the matrix effects using an internal standard and a relative sensitivity factor (RSF) to calculate the final analyte concentration. This requires shorter analysis time and saves space in the ablation chamber, but different mathematical calculations are required. This method can be considered semi-quantitative because it may be limited in accuracy and precision and, therefore, only used as a quantitative pre-analysis method [27, 28]. In fact, this method was presented and validated for quantification of different trace elements, such as Pb and Ba, using different geologically certified reference materials (CRM), such as NIST 612, for RSF calculation [27].

In 2012, Jochum et al. also applied one-point calibration using CRMs for RSF calculation but in stalagmite and

shell analysis, in which they determined concentrations of 30–50 trace elements (such as Ca, Pb, Mg, Zn, Sr, and Ba), with uncertainties ranging from 5 to 10%. In the study, the authors reported the need for materials to be compatible with the matrix of interest, in addition to CRMs, because some elements with low boiling points, such as Pb, require calibration points for matrix compatibility, in order to decrease the uncertainties in the analysis [29].

The literature reports different applications for this calibration method. For example, using CRM as the analytical point and carrier gas as the analytical ‘blank’, Hare et al. (2011) quantified Zn, Sr, Pb, and Cd in teeth via quantitative imaging by LA-ICP-MS. The results showed that Sr and Zn were quantified in the range of 80–300 $\mu\text{g g}^{-1}$ and Cd and Pb were 30–300 ng g^{-1} for different regions of the sample [30]. Moradi et al. (2010) used CRM from olive leaves to quantify Ni and Fe in *Berkheya coddii* root sections, and to map the dimethylglyoxime (Ni-DMG) complex on the root surface. The results showed high Ni concentrations inside the root (ca. 500 mg kg^{-1} in the cortex and 300 mg kg^{-1} in the root centre), with Fe concentrations lower than 100 mg kg^{-1} , confirmed by decomposition and ICP optical emission spectroscopy (OES) [31].

Santos et al. (2009) also applied this method to quantify Cu, Zn, Cd, Hg, and Pb in sea snail tissue samples, using CRM to calculate the RSF for subsequent imaging in LA-ICP-MS via analytical curves, and no significant differences (at a 95% confidence level) were found between the values from one-point and ICP-MS methods [28].

Hare et al. (2012) noted that the term ‘semi-quantitative’ should be avoided because calibration methods are classified either as being ‘quantitative’, in which the figures of merit (i.e. analytical recovery, detection, and quantification limits) are present, or as ‘qualitative’ [32]. According to the International Union of Pure and Applied Chemistry (IUPAC), for methods using a calibration point, the limits of detection (LOD) and quantification (LOQ) can be obtained based on the standard deviation of the blank (σ) of the analysis [33–35]. Therefore, the one-point calibration strategy can be classified as a quantitative method.

Therefore, this work aims to evaluate two quantitative methods based on the external calibration applied in LA-ICP-MS analysis: (i) the analytical curve and (ii) the one-point. Both methods use the matrix-matching concept to quantify three PTEs (Pb, Cd, and Ba) in CRM and environmental homogeneity in wood samples. The standard sample preparation from matrix matching was also evaluated to provide the highest homogeneity and signal intensity to the LA-ICP-MS analysis. In the literature, the one-point calibration strategy has not been reported for wood samples but could be a welcome alternative to the conventional quantitative method which is usually applied.

Materials and methods

Chemicals and reagents

For acid digestion of the sample, twice sub-distilled nitric acid (HNO_3) (Merck, Darmstadt, Germany), hydrogen peroxide (H_2O_2) (Merck, Darmstadt, Germany), and deionised water ($18 \text{ M}\Omega \text{ cm}^{-1}$; Millipore, Bedford, MA, USA) were used. An analytical standard solution of Pb, Cd, and Ba (Tec Lab, 1000 $\mu\text{g g}^{-1}$) was used to prepare the in-house calibration pressed pellets.

Pellet sample preparation

For the preparation of in-house pressed pellets to perform the external calibration, a sample of *Pinus taeda* wood was crushed in a ball mill (Gerhard Koch) and sieved to obtain particle sizes smaller than 75 μm . A 5-g sample was cleaned with 60 mL of 0.2 mol L^{-1} HNO_3 under magnetic agitation in a vacuum filtration system (six times) to remove impurities and metals from the composition of the wood. It was then washed with deionised water and dried at 37 $^\circ\text{C}$, until a constant weight was maintained [36].

LA-ICP-MS analysis

A New Wave Research UP-213 laser ablation system with a Nd:YAG (213 nm) laser source coupled to a quadrupole ICP-MS (PerkinElmer ELAN DRC-e) was used to monitor $^{13}\text{C}^+$, $^{206}\text{Pb}^+$, $^{208}\text{Pb}^+$, $^{112}\text{Cd}^+$, $^{114}\text{Cd}^+$, $^{137}\text{Ba}^+$, and $^{138}\text{Ba}^+$ in tree rings and calibration samples. Initially, a daily analysis, using a solution of Mg, In, Be, Ce, and U, was applied to evaluate the operational conditions of the ICP-MS and check the production of oxide, double-charge, and mono-charge species, which must be present in values below 3%. The data acquisition was carried out after 45 min of argon plasma stabilisation and monitoring of the ^{13}C signal intensity. The ablated sample mass was transported towards the ICP using argon (Ar) as the carrier gas. All LA-ICP-MS measurements were performed in a class 10,000 cleanroom. The laser ablation acquisition was made in line scan mode with a 60 $\mu\text{m s}^{-1}$ scan speed. To correct and compensate for possible instrumental oscillation, ^{13}C was used as an internal standard in all analytical signal intensity measurements during the ablation process. All the instrumental and analytical parameters were optimised and are summarised in Table 1. It is important to highlight that the analytical signal-to-background signal ratio (SBR) and background signal equivalent concentration (BEC) parameters were also evaluated in order to obtain

Table 1 Optimised instrumental operational conditions and measurement by LA-ICP-MS for wood analysis

| ICP-MS (PerkinElmer ELAN DRC-e) | |
|---|--------------|
| RF power (W) | 1300 |
| Nebuliser gas flow (L min ⁻¹) | 1.2 |
| Auxiliary gas flow (L min ⁻¹) | 1.6 |
| Data acquisition parameters | |
| Reading mode | Peak hopping |
| Detector mode | Dual |
| Sweeps | 3 |
| Dwell time (ms) | 20 |
| Integration time (ms) | 60 |
| LA (New Wave UP-213) | |
| Nd:YAG (nm) | 213 |
| Laser ablation intensity (%) | 70 |
| Frequency (Hz) | 20 |
| Spot size (μm) | 110 |
| Scan speed (μm s ⁻¹) | 60 |
| Average energy pulse (mJ) | 1.21 |
| Average fluence (J cm ⁻²) | 16.69 |

higher SBR and lower BEC values and provide less background signal and not negatively influence the analysis, as mentioned and shown in the previously published article by Amais et al. (2021) [37].

All mass spectrometer data treatment and analysis were performed using Microsoft Office Excel 2010 (Microsoft Corporation).

Pellet preparation: evaluation of elemental homogeneity

To verify the process for the preparation of pressed pellets for calibration, values of relative standard deviation (RSD, %) and elemental signal intensity (counts per second, cps) were evaluated from the LA-ICP-MS results. In this case, two different cellulose pellets (Vetec) were prepared, with 25 μg g⁻¹ of Pb, Cd, and Ba, and taking two different preparation processes into account.

For process A [22], 0.2 g of sample was spiked with 400 μL of a standard solution containing the element of interest, dried for 72 h at 37 °C, and homogenised with a pestle and mortar for 10 min.

For process B [38], 0.2 g of sample was placed in a Falcon tube, in which 1.2 mL of a 1% HNO₃ solution of known analytical concentrations was added. The mixture was then vortexed for 2 min, frozen with liquid nitrogen, and freeze-dried (Virtis) for 72 h.

After drying, the sample from each process A and B was homogenised for 4 min with a vortex and pressed in a digital hydraulic press (PIKE CrushIR) for 1 min; 7 ton cm⁻² was applied to prepare the disc pellets. The LA-ICP-MS analysis

was performed using three 6-mm scan lines, with a 0.110-mm spot diameter and 1.6 mm distance between each centre of the line, according to the analytical parameters described in Table 1.

LA-ICP-MS external calibration strategies

The analysis by LA-ICP-MS was performed by applying five parallel line scans with a distance of 0.24 mm between each centre of the line, line size of 1.5 mm, and laser spot diameter of 110 μm. For the analytical validation procedure, the certified values of 1575a—Trace Elements in Pine Needles (*Pinus taeda*), 1547—Peach leaves, and BCR 414—Plankton reference materials were used to evaluate the LOD, LOQ, recovery (%), and RSD, according to IUPAC [34, 35].

Strategy 1: analytical curve

The analytical curve, based on the matrix-matching (in-house pellets) concept, was prepared with a *P. taeda* sample after cleaning. In this case, five points with different concentrations (0.0, 0.2, 1.0, 5.0, and 25.0 μg g⁻¹) were prepared for Pb, Cd, and Ba, according to process B, as described in the “[Pellet preparation: evaluation of elemental homogeneity](#)” section. The elemental concentrations were determined through a linear equation, $y \text{ (cps)} = ax \text{ (}\mu\text{g g}^{-1}\text{)} + b$ (where ‘a’ is the angular coefficient and ‘b’ is the linear coefficient). The ¹³C isotope was used as an internal standard. The LOD and LOQ were determined as $(3 \times s_{\text{blank}})/b$ and $(10 \times s_{\text{blank}})/b$, respectively, where s_{blank} is the standard deviation of analytical blank measurements and b is the slope of the analytical curve. The RSD values were obtained from the ratio between the standard deviation from the element’s signal intensity (or elemental concentration) and the medium values.

Strategy 2: one-point calibration

In the case of one-point calibration, matrix-matched in-house pellets were prepared with 1.0, 5.0, and 25.0 μg g⁻¹ of Pb, Cd, and Ba in a *P. taeda* sample, according to process B, as described in the “[Pellet preparation: evaluation of elemental homogeneity](#)” section. Quantification analysis via one-point calibration [27, 28] requires the values of the internal standard concentration and the relative sensitive factor (RSF) to be known, which are obtained by Eq. 1:

$$RSF = \frac{C_{ap}}{C_{true, std}} \quad (1)$$

where $C_{true, std}$ is the certified elemental concentration, and C_{ap} is the apparent elemental concentration in the CRM/in-house pellet. The C_{ap} is given by Eq. 2:

$$C_{ap} = C_{IS} \times \frac{I_e}{I_{IS}} \times \left[\frac{\left(\frac{A_{IS}}{A_e} \right)}{\left(\frac{M_e}{M_{IS}} \right)} \right] \tag{2}$$

where C_{IS} is the internal standard concentration ($\mu\text{g g}^{-1}$), I_e , A_e , and M_e are the signal intensity, isotopic abundance, and relative atomic mass of the element of interest, respectively, and I_{IS} , A_{IS} , and M_{IS} are related to the internal standard. In this case, the concentration of carbon was considered to be $5.10^5 \mu\text{g g}^{-1}$ for all samples analysed, because of the similarity between the signal intensity from each sample [39]. Thus, to obtain the final concentration C of the element of interest, it was necessary to apply Eq. 3:

$$C (\mu\text{g g}^{-1}) = C_{ap} \times \frac{1}{RSF} \tag{3}$$

Application in a wood sample

For the analysis of elemental concentration in wood, two samples of *Tipuana tipu* (Benth.) Kuntze (Fabaceae) were collected in São Paulo City (Brazil), crushed using an IKA T 10 basic Ultra-Turrax® (Staufeb im Breisgau, Germany) for 1 min, and milled using a cryogenic mill (Freezer/Mill 6870, Spex Sample Prep). Milling was carried out in five cycles, with 5 min precooling time, 2 min run time, and 1 min cooling time at a rate of 15 cps. The samples were pressed in a digital hydraulic press (PIKE CrushIR) for 1 min at 7 ton cm^{-2} , to prepare the disc pellets for LA-ICP-MS analysis. More detailed sampling and environmental information can be found in Locosselli et al. (2018) [2].

To validate the LA-ICP-MS analysis, 50 mg of the sample was subjected to acid digestion with 7 mL of 37.5% (v/v) nitric acid (HNO_3), 25% (v/v) of hydrogen peroxide (H_2O_2), and deionised water solution in a microwave (Berg-hof, Speedwave® DIRC, Germany) in a closed Teflon® tube. The mixtures were subjected to the following microwave program: 5 min at 400 W; 15 min at 500 W; 4 min at 320 W; and 3 min at 0 W. After acid digestion, the solutions were analysed using ICP-MS (ICPMS-2030, Shimadzu, Japan), with He as the collision cell gas.

Results and discussion

Evaluation of elemental homogeneity for pellet preparation

In this work, two types of pellet sample preparation were applied in order to determine which process provided the highest signal intensity and lowest RSD from each isotope measured by LA-ICP-MS. Process A was carried out using

a pestle and mortar to homogenise the sample, which also helped to decrease particle size and promote the removal of greater amounts of particles during the ablation process, thus increasing the signal intensity of the analytes [18, 24]. Process B was carried out using the freeze-drying process, which consists of sublimation of water, helping to preserve the chemical constituents by drying under a partial vacuum and contributing to the homogeneity of the solid particles [40]. The elemental profile from both sample preparation processes is presented in Fig. 1.

When evaluating the sample preparation processes, it can be seen that they both enable the linear behaviour of the isotopes under analysis, i.e. the elemental homogeneity of the pellets through the ablation profile. However, process A showed higher RSD values, as seen in Table 2, which indicates higher oscillations in the analytical signals caused by

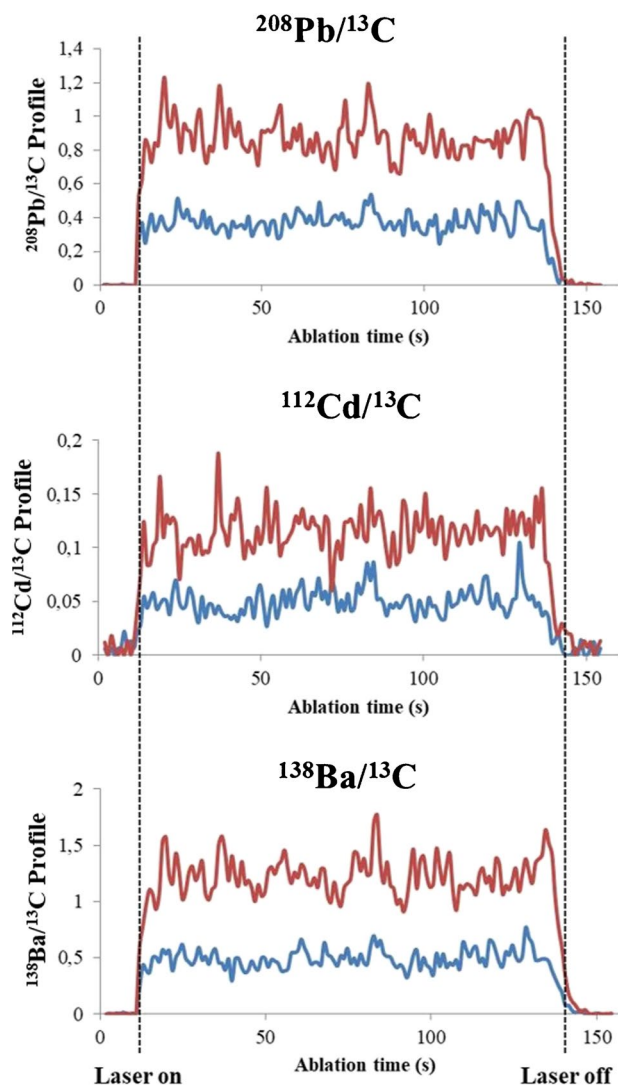


Fig. 1 Elemental profile from sample preparation process A (blue line) and process B (red lines)

Table 2 Elemental homogeneity from different pellet sample preparation processes

| | | $^{208}\text{Pb}/^{13}\text{C}$ | $^{206}\text{Pb}/^{13}\text{C}$ | $^{112}\text{Cd}/^{13}\text{C}$ | $^{114}\text{Cd}/^{13}\text{C}$ | $^{137}\text{Ba}/^{13}\text{C}$ | $^{138}\text{Ba}/^{13}\text{C}$ |
|-----------|---------|---------------------------------|---------------------------------|---------------------------------|---------------------------------|---------------------------------|---------------------------------|
| Process A | Average | 0.39 | 0.18 | 0.05 | 0.06 | 0.08 | 0.51 |
| | RSD (%) | 5.3 | 5.9 | 8.0 | 7.1 | 4.7 | 7.8 |
| Process B | Average | 0.85 | 0.40 | 0.11 | 0.14 | 0.18 | 1.18 |
| | RSD (%) | 2.8 | 2.3 | 1.1 | 1.4 | 3.1 | 2.7 |

Average analyte/IS (n = 3 lines)

lower homogeneity. In addition, higher detectability for all analytes is observed in process B than in process A, which may indicate the highest efficiency in pellet preparation, with minimum loss of the analytes and greater assimilation of the analytes in the matrix, since the freeze-drying process is widely used to preserve components in a sample through the sublimation process, especially as applied in the food industry [41].

In addition to the increased analytical signal and low RSD values, process B offers a shorter sample preparation time, making it more feasible for pellet production for analysis by LA-ICP-MS. Therefore, it was chosen to prepare the pellets to be used in both external curve calibration and one-point calibration.

LA-ICP-MS calibration strategies

Calibration strategy 1

The analytical curve using matrix matching was constructed by preparing six points of known concentration of each analyte. As can be seen in Table 3, all analytical curves show an adequate correlation between elemental concentration and analyte/IS ($R > 0.999$), as well as low LOD and LOQ, which are important results, as the analytes are PTEs for wood samples.

The analytical recovery results (Table 4) show adequate values (> 70%), and precise results were also obtained through RSDs (up to 10–15%), ensuring an accurate and precise analytical method [42]. However, even with the improvement in limits of quantification, the concentrations of Pb isotopes and ^{112}Cd in CRM pine needles (a similar wood matrix) are below the LOQ. It is worth noting that the Pb concentration in this material is not certified, which may

also influence the results, since this value cannot be taken into account for calibration methods. In this case, to ensure the accuracy and precision of the quantification method, tests were also performed with different certified reference materials, such as peach leaves and plankton CRMs, which presented concentrations obtained above the LOQ of the analytical curve. All the results can be seen in Table 4, confirming that the quantification method has recoveries of > 74.8% and RSD < 15.9% for the analytes of interest. The isotope ^{112}Cd in the plankton sample shows 28.7% as the RSD value, and this matrix is less similar than those for performing the quantification points via one-point, which could be the cause of the matrix effect in the analysis via LA-ICP-MS, as well as transport effects due to laser oscillations and aerosol dispersion into the ICP-MS transport [43]. It is worth mentioning that the certified values are correlated with the total concentration from each element, and not with the isotopic composition, so variations between the responses of each isotope can occur according to the natural abundance.

Although the analytical curve by matrix-matching concept can be considered an efficient quantification method by LA-ICP-MS determination, an excessive analysis time (ca. 90 min), taking into account the total ablation process and the manual laser focus required, can be a drawback.

Calibration strategy 2

The use of a certified reference material as an analytical point for calculating the RSF is observed in the literature [28, 29] when considering the one-point calibration method. However, it is also commonly known that the CRM does not match the diversity of matrices, which is a serious limitation for quantitative analysis via LA-ICP-MS. The present study sought to apply the

Table 3 Results obtained for the analytical curve and matrix-matching concept by LA-ICP-MS

| Isotope | $y = ax + b$ | LOD ($\mu\text{g g}^{-1}$) | LOQ ($\mu\text{g g}^{-1}$) | R |
|---------------------------------|-------------------------|------------------------------|------------------------------|--------|
| $^{206}\text{Pb}/^{13}\text{C}$ | $y = 0.0222x + 0.00005$ | 0.053 | 0.176 | 0.9999 |
| $^{208}\text{Pb}/^{13}\text{C}$ | $y = 0.04786x - 0.0004$ | 0.068 | 0.227 | 0.9999 |
| $^{112}\text{Cd}/^{13}\text{C}$ | $y = 0.0091x + 0.00021$ | 0.064 | 0.215 | 0.9999 |
| $^{114}\text{Cd}/^{13}\text{C}$ | $y = 0.01141x - 0.0003$ | 0.045 | 0.151 | 0.9999 |
| $^{137}\text{Ba}/^{13}\text{C}$ | $y = 0.0086x - 0.0002$ | 0.084 | 0.280 | 0.9999 |
| $^{138}\text{Ba}/^{13}\text{C}$ | $y = 0.0557x - 0.0008$ | 0.056 | 0.186 | 0.9997 |

Table 4 Experimental concentration, recovery, and RSD obtained from CRM pine needles, peach leaves, and plankton by LA-ICP-MS analytical curve

| CRM pine needles | | | | |
|---------------------------------|------------------------------------|---------------------------------------|--------------|---------|
| Isotope/IS | Certified ($\mu\text{g g}^{-1}$) | Experimental ($\mu\text{g g}^{-1}$) | Recovery (%) | RSD (%) |
| $^{206}\text{Pb}/^{13}\text{C}$ | 0.167 | 0.13 ± 0.02 | <LOQ | 15.9 |
| $^{208}\text{Pb}/^{13}\text{C}$ | 0.167 | 0.12 ± 0.01 | <LOQ | 5.3 |
| $^{112}\text{Cd}/^{13}\text{C}$ | 0.233 | 0.19 ± 0.01 | <LOQ | 7.5 |
| $^{114}\text{Cd}/^{13}\text{C}$ | 0.233 | 0.20 ± 0.01 | 88.8 | 6.6 |
| $^{137}\text{Ba}/^{13}\text{C}$ | 6 | 4.6 ± 0.2 | 76.8 | 4.7 |
| $^{138}\text{Ba}/^{13}\text{C}$ | 6 | 4.5 ± 0.3 | 74.8 | 6.4 |
| CRM peach leaves | | | | |
| Isotope/IS | Certified ($\mu\text{g g}^{-1}$) | Experimental ($\mu\text{g g}^{-1}$) | Recovery (%) | RSD (%) |
| $^{206}\text{Pb}/^{13}\text{C}$ | 0.869 | 0.74 ± 0.02 | 85.2 | 3.5 |
| $^{208}\text{Pb}/^{13}\text{C}$ | 0.869 | 0.69 ± 0.04 | 80.3 | 5.8 |
| $^{112}\text{Cd}/^{13}\text{C}$ | n | n | n | n |
| $^{114}\text{Cd}/^{13}\text{C}$ | n | n | n | n |
| $^{137}\text{Ba}/^{13}\text{C}$ | 123.7 | 111 ± 2 | 90.2 | 2 |
| $^{138}\text{Ba}/^{13}\text{C}$ | 123.7 | 112 ± 2 | 90.8 | 2 |
| CRM plankton | | | | |
| Isotope/IS | Certified ($\mu\text{g g}^{-1}$) | Experimental ($\mu\text{g g}^{-1}$) | Recovery (%) | RSD (%) |
| $^{206}\text{Pb}/^{13}\text{C}$ | 3.97 | 3.1 ± 0.2 | 77.5 | 7.2 |
| $^{208}\text{Pb}/^{13}\text{C}$ | 3.97 | 3.2 ± 0.2 | 80.0 | 7.6 |
| $^{112}\text{Cd}/^{13}\text{C}$ | 0.383 | 0.3 ± 0.1 | 78.2 | 28.7 |
| $^{114}\text{Cd}/^{13}\text{C}$ | 0.383 | 0.35 ± 0.04 | 92.0 | 11.3 |
| $^{137}\text{Ba}/^{13}\text{C}$ | n | n | n | n |
| $^{138}\text{Ba}/^{13}\text{C}$ | n | n | n | n |

n = certified concentration not provided

Table 5 Relative sensitive factor (RSF) values from *P. taeda* lyophilised pellets

| Isotope | RSF | | |
|-------------------|------------------------|------------------------|-------------------------|
| | $1 \mu\text{g g}^{-1}$ | $5 \mu\text{g g}^{-1}$ | $25 \mu\text{g g}^{-1}$ |
| ^{206}Pb | 30.4 ± 2.6 | 28.2 ± 7.1 | 29.5 ± 1.5 |
| ^{208}Pb | 29.5 ± 2.7 | 27.9 ± 7.0 | 29.2 ± 1.5 |
| ^{112}Cd | 22.0 ± 2.4 | 21.9 ± 5.7 | 22.2 ± 1.2 |
| ^{114}Cd | 22.8 ± 1.4 | 17.9 ± 11.1 | 23.4 ± 1.1 |
| ^{137}Ba | 36.4 ± 3.2 | 35.3 ± 9.2 | 36.8 ± 2.4 |
| ^{138}Ba | 35.1 ± 1.3 | 34.4 ± 10.1 | 37.5 ± 2.7 |

matrix-matching concept (*P. taeda*) for the preparation of three analytical points of known concentrations ($1, 5,$ and $25 \mu\text{g g}^{-1}$) to perform the RSF calculations (Eq. 1 in the “Strategy 2: one-point calibration” section). This should correct differences in the formation, transmission, and detection of element ions (known as the matrix effect), as well as mass fractionation effects [27], once it is considered as a correction factor. This is calculated by the ratio between the apparent concentration (obtained by LA-ICP-MS, Eq. 2 in the “Strategy 2: one-point calibration” section) and the certified concentration (Eq. 1). The RSF results are presented in Table 5.

Equation 2 is used to calculate the apparent concentration because the RSF values are known; the final concentration values (Eq. 3) are then found for each isotope in the CRM of pine needles. The final concentration results, as well as the relative recovery (%) and RSD for each analytical point evaluated, are presented in Table 6. As for the analytical curve, quantification was also performed by employing peach leaves and plankton as the CRMs to ensure the precision and accuracy results for the one-point calibration method. The certified concentration of each analyte and the CRM samples can be seen in Table 4 (“Calibration strategy 1” section).

In addition to the values obtained by the analytical curve, the final concentrations are consistent with the certified values, in which only the recovery of the ^{208}Pb isotope, at the point of $1 \mu\text{g g}^{-1}$, is below the range considered optimal; the other isotopes for the three points evaluated present analytical recovery above 70%. The RSD values are in the expected range (below 10–15%), thus ensuring the accuracy of the one-point calibration method. In this case, the analytical point concentration of $5 \mu\text{g g}^{-1}$ showed the best analytical recovery values, as well as RSD below the limit (10–15%), ensuring precision and accuracy. The ^{112}Cd isotope showed imprecise results for the CRM samples (RSD > 26.7%), considering the three analytical points evaluated, similar to

Table 6 Results obtained by one-point calibration and matrix matching by LA-ICP-MS

| 1 µg g⁻¹ | | | | | | | | | |
|-----------------------------|---------------------------------|-----------------|-------------------------|---------------------------------|-----------------|---------------------|---------------------------------|-----------------|----------------|
| CRM Pinus Needles | | | CRM Peach Leaves | | | CRM Plankton | | | |
| | Exp. (µg g⁻¹) | Rec. (%) | RSD (%) | Exp. (µg g⁻¹) | Rec. (%) | RSD (%) | Exp. (µg g⁻¹) | Rec. (%) | RSD (%) |
| ²⁰⁶ Pb | 0.12 ± 0.02 | <LOQ | 15.6 | 0.72 ± 0.02 | 82.8 | 3.5 | 2.98 ± 0.21 | 75.1 | 7.2 |
| ²⁰⁸ Pb | 0.113 ± 0.006 | <LOQ | 5.7 | 0.68 ± 0.04 | 78.4 | 5.9 | 3.1 ± 0.2 | 78.8 | 7.6 |
| ¹¹² Cd | 0.22 ± 0.01 | <LOQ | 6.7 | n | n | n | 0.33 ± 0.08 | 85.0 | 26.7 |
| ¹¹⁴ Cd | 0.18 ± 0.01 | 79.2 | 7.6 | n | n | n | 0.33 ± 0.04 | 87.0 | 12.2 |
| ¹³⁷ Ba | 4.5 ± 0.3 | 75.2 | 7.5 | 112 ± 2 | 91.2 | 2 | n | n | n |
| ¹³⁸ Ba | 4.8 ± 0.3 | 79.5 | 6.4 | 119 ± 2 | 96.7 | 2 | n | n | n |
| 5 µg g⁻¹ | | | | | | | | | |
| CRM Pinus Needles | | | CRM Peach Leaves | | | CRM Plankton | | | |
| | Exp. (µg g⁻¹) | Rec. (%) | RSD (%) | Exp. (µg g⁻¹) | Rec. (%) | RSD (%) | Exp. (µg g⁻¹) | Rec. (%) | RSD (%) |
| ²⁰⁶ Pb | 0.13 ± 0.02 | <LOQ | 15.6 | 0.77 ± 0.03 | 89.2 | 3.5 | 3.2 ± 0.2 | 81.0 | 7.2 |
| ²⁰⁸ Pb | 0.12 ± 0.01 | <LOQ | 5.7 | 0.73 ± 0.04 | 82.7 | 6.1 | 3.3 ± 0.2 | 83.2 | 7.6 |
| ¹¹² Cd | 0.22 ± 0.01 | <LOQ | 6.7 | n | n | n | 0.32 ± 0.09 | 85.2 | 26.7 |
| ¹¹⁴ Cd | 0.23 ± 0.02 | 100.8 | 7.6 | n | n | n | 0.42 ± 0.05 | 110.8 | 12.2 |
| ¹³⁷ Ba | 4.8 ± 0.2 | 79.7 | 4.7 | 116 ± 2 | 94.1 | 2 | n | n | n |
| ¹³⁸ Ba | 4.9 ± 0.2 | 82.7 | 5.3 | 122 ± 2 | 98.7 | 2 | n | n | n |
| 25 µg g⁻¹ | | | | | | | | | |
| CRM Pinus Needles | | | CRM Peach Leaves | | | CRM Plankton | | | |
| | Exp. (µg g⁻¹) | Rec. (%) | RSD (%) | Exp. (µg g⁻¹) | Rec. (%) | RSD (%) | Exp. (µg g⁻¹) | Rec. (%) | RSD (%) |
| ²⁰⁶ Pb | 0.12 ± 0.01 | <LOQ | 10.3 | 0.75 ± 0.04 | 85.8 | 5.1 | 2.99 ± 0.06 | 75.4 | 2.2 |
| ²⁰⁸ Pb | 0.115 ± 0.001 | <LOQ | 1.2 | 0.68 ± 0.03 | 78.6 | 4.6 | 3.16 ± 0.21 | 79.7 | 6.6 |
| ¹¹² Cd | 0.22 ± 0.02 | <LOQ | 9.7 | n | n | n | 0.32 ± 0.07 | 83.1 | 22.8 |
| ¹¹⁴ Cd | 0.182 ± 0.009 | 78.0 | 5 | n | n | n | 0.33 ± 0.03 | 85.0 | 10.4 |
| ¹³⁷ Ba | 4.7 ± 0.3 | 78.7 | 5.8 | 114 ± 3 | 92.2 | 2.9 | n | n | n |
| ¹³⁸ Ba | 4.713 ± 0.005 | 78.5 | 8.8 | 114 ± 4 | 92.6 | 3.9 | n | n | n |

n = certified concentration not provided

Table 7 LOD and LOQ for one-point method using a blank standard pellet

| Isotope | LOD (µg g ⁻¹) | LOQ (µg g ⁻¹) |
|-------------------|---------------------------|---------------------------|
| ²⁰⁶ Pb | 0.048 | 0.145 |
| ²⁰⁸ Pb | 0.074 | 0.226 |
| ¹¹² Cd | 0.072 | 0.220 |
| ¹¹⁴ Cd | 0.064 | 0.193 |
| ¹³⁷ Ba | 0.078 | 0.235 |
| ¹³⁸ Ba | 0.058 | 0.176 |

analytical curve results (Table 4 in the “Calibration strategy 1” section).

In considering the one-point calibration method, the LOD and LOQ were calculated using the standard deviation of the ratio between the intensity of the isotopes and the internal standard from blank pellet analysis [34, 35]. The results can be seen in Table 7, which shows similar LOD and LOQ values to those obtained by the analytical curve (Table 3, “Calibration strategy 1” section).

In the literature, one-point calibration is considered a semi-quantitative method because it is limited in accuracy and precision [28]. However, through the results described in this article, this method can be applied for quantitative purposes involving LA-ICP-MS in wood samples. It is also worth noting that the analytical points evaluated are in the linear range of the analytical curve ($R > 0.99$), corroborating the promising results observed in the total quantification of the isotopes evaluated. In addition, such a method is less time-consuming once it uses only one calibration point; the analysis is performed in less than 15 min (depending on the LA-ICP-MS parameters).

As already discussed in this work, there are some pros and cons in using each strategy, but it should be noted that minimisation strategies [21] should always be sought in an analytical method, whilst preserving all the analytical figures, such as accuracy, precision, and time consumption. We have shown that the one-point calibration method presented the best analytical recovery values and lowest RSD values for the isotopes under study.

Table 8 LA-ICP-MS analytical curve and one-point calibration results for wood samples and validation by ICP-MS solution

| | Sample 1 | | | | Sample 2 | | |
|-------------------|--|--|-------|------------------------|---|-------|------------------------|
| | ICP-MS Concentration ($\mu\text{g g}^{-1}$) | Analytical curve (LA-ICP-MS) Concentration ($\mu\text{g g}^{-1}$) | | Student <i>t</i> -test | One-point (LA-ICP-MS) Concentration ($\mu\text{g g}^{-1}$) | | Student <i>t</i> -test |
| ²⁰⁶ Pb | 0.71 ± 0.02 | 0.77 ± 0.13 | 108.5 | 0.163* | 0.77 ± 0.08 | 108.5 | 0.60** |
| ²⁰⁸ Pb | 0.72 ± 0.01 | 0.73 ± 0.13 | 101.4 | 0.79* | 0.73 ± 0.04 | 101.4 | 1.172** |
| ¹¹² Cd | 0.337 ± 0.004 | 0.72 ± 0.10 | 211.8 | 6.846* | 0.75 ± 0.10 | 220.6 | 7.285* |
| ¹¹⁴ Cd | 0.34 ± 0.01 | 0.76 ± 0.06 | 223.5 | 12.838* | 0.77 ± 0.06 | 226.5 | 12.75* |
| ¹³⁷ Ba | 2.13 ± 0.02 | 2.44 ± 0.05 | 114.6 | 9.845** | 2.65 ± 0.05 | 124.4 | 15.327** |
| ¹³⁸ Ba | 2.62 ± 0.04 | 2.69 ± 0.04 | 102.7 | 2.281** | 2.76 ± 0.19 | 105.3 | 1.290* |
| | ICP-MS Concentration ($\mu\text{g g}^{-1}$) | Analytical curve (LA-ICP-MS) Concentration ($\mu\text{g g}^{-1}$) | | Student <i>t</i> -test | One-point (LA-ICP-MS) Concentration ($\mu\text{g g}^{-1}$) | | Student <i>t</i> -test |
| ²⁰⁶ Pb | 0.49 ± 0.01 | 0.37 ± 0.03 | 75.5 | -6.366** | 0.47 ± 0.03 | 95.9 | -0.775** |
| ²⁰⁸ Pb | 0.50 ± 0.01 | 0.38 ± 0.02 | 76.0 | -9.098** | 0.47 ± 0.02 | 94.0 | -2.25** |
| ¹¹² Cd | 0.34 ± 0.01 | 0.33 ± 0.01 | 97.1 | -1.916** | 0.34 ± 0.01 | 100.0 | 0.051** |
| ¹¹⁴ Cd | 0.357 ± 0.005 | 0.361 ± 0.002 | 101.1 | -1.252** | 0.359 ± 0.002 | 100.6 | -0.655** |
| ¹³⁷ Ba | 1.86 ± 0.06 | 2.25 ± 0.02 | 121.0 | -9.846** | 2.44 ± 0.03 | 131.2 | -14.53** |
| ¹³⁸ Ba | 2.18 ± 0.02 | 2.32 ± 0.05 | 106.4 | 4.378** | 2.47 ± 0.06 | 113.3 | 8.697** |

t*-critical ($p > 0.05$): 4,303*t*-critical ($p > 0.05$): 2,776

n = 3

PTE quantification in environmental wood samples

As mentioned above, tree rings are widely used as proxies for monitoring climate change because they can incorporate elements present in the air and soil [1, 2, 37]. However, there is no environmental law that can be used to verify minimum concentrations of PTEs in this type of sample, which directly impacts its application in quantitative environmental analysis. In this context, two samples of *Tipuana tipu* (Benth.) Kuntze (Fabaceae) were used to apply the quantitative strategies evaluated in this article. These samples were studied by Locosselli et al. (2018), and a qualitative decrease in Cd and Pb along the tree rings was observed, which was attributed to the reduction in environmental pollution in São Paulo City [2].

In the literature, it is mentioned that heterogeneity between growth rings can negatively influence the comparison between quantitative LA-ICP-MS and ICP-MS results [25, 44]. Therefore, in order to evaluate the applicability of the quantitative method, the tree ring samples were ground and prepared as discussed in the “Application in wood sample” section, in order to obtain homogeneous samples and minimise the effect of sample heterogeneity on the analyses performed.

In this case, the analytical curve and the $5 \mu\text{g g}^{-1}$ one-point calibration were applied to two pellet samples from the *Tipuana tipu* species. Considering the matrix-matching

concept, the difference between wood species from the calibration pellet and the sample pellet does not negatively impact the analysis, as they are similar matrices and will interact similarly with laser ablation, minimising the matrix effect [13, 23]. To validate the results by recovery (%), each sample was subjected to acid digestion and analysed by ICP-MS; the results were considered to be the real concentration. Table 8 presents all of the quantitative results by ICP-MS, analytical curve, and one-point by LA-ICP-MS for Pb, Cd, and Ba, as well as the recovery and *t*-test values.

It was observed that both calibration strategies provided similar results and can be compared to those obtained by ICP-MS, thus demonstrating the applicability of the one-point calibration strategy in quantifying PTEs in wood samples, which can corroborate environmental analysis without involving the loss of the sample in the digestion step. Differences between the *t*-test results for Cd and ¹³⁷Ba isotopes in sample 1 and Pb and Ba isotopes in sample 2 were observed, compared to the ICP-MS concentrations providing adequate accuracy. The differences between Cd results can be correlated with differences between the sampling by LA-ICP-MS and the ICP-MS sample introduction because the LA-ICP-MS analysed micro-regions at the sample surface, which could show micro-hotspots in the elemental concentrations that are lost during the acid digestion but affect the LA-ICP-MS accuracy and precision results. The difference between the species from the wood sample pellets (*Tipuana tipu*)

and the standard pellets (*P. taeda*) can also influence the laser analysis by matrix and transport effects [13]. Similar results are observed in the literature by Moreau and Arruda (2022) when comparing Zn and Cu concentrations in tomato leaves CRM (1573a) [25]. Between 135 and 150% recovery was achieved using qualitative filter paper as a solid support to calibration points [25]. Loni et al. (2019) also found no agreement between Hg concentration in tree ring samples from *Quercus petraea* species, comparing LA-ICP-MS and ICP-MS acid digestion results, in which the LA results were overestimated [44].

Conclusions

The main objective of this work was successfully attained. According to the results obtained in the total quantification of Pb, Cd, and Ba in samples of *Tipuana tipu*, it can be concluded that both of the methods studied are efficient and amenable to application in quantitative LA-ICP-MS. While comparing the methods, it was found that the one-point method presented the best values of analytical recovery, the lowest RSD values for the isotopes under study, and the shortest time taken, when compared with the analytical curve in LA-ICP-MS quantification. Therefore, the one-point method can be considered exact and precise for quantitative applications in homogeneous wood samples.

Acknowledgements The authors are grateful to Daigard R. Ortega Rodriguez, Prof. Dr Mario Tomazello-Filho and Prof. Dr Giuliano M. Locosselli of University São Paulo (Piracicaba, SP, Brazil) for providing the *T. tipu* samples from São Paulo (Brazil) city and the *P. taeda* samples. We also thank Prof. Marcelo Ganzarolli (Institute of Chemistry at University of Campinas) for the use of the freeze-drying equipment.

Funding This work was financial supported by Fundação de Amparo à Pesquisa do Estado de São Paulo (FAPESP 2014/50867-3, 2017/50085-3, 2018/25207-0, 2019/00063-9, 2019/24445-8, and 2020/08543-7), and Conselho Nacional de Desenvolvimento Científico e Tecnológico (CNPq 303231/2020-3).

Declarations

Conflicts of interest The authors declare that they have no competing interests. The funders had no role in the design of the study; in the collection, analyses, or interpretation of data; in the writing of the manuscript, or in the decision to publish the results.

References

- Burns SJ, Welsh LK, Scropton N, Cheng H, Edwards RL. Millennial and orbital scale variability of the South American Monsoon during the penultimate glacial period. *Sci Rep*. 2019;9:4–8. <https://doi.org/10.1038/s41598-018-37854-3>.
- Locosselli GM, Chaccon-Madrid K, Arruda MAZA, Camargo EP, Moreira TCL, Singer JM, André PA, André CDS, Buckeridge MS. Tree rings reveal the reduction of Cd, Cu, Ni and Pb pollution in the central region of São Paulo, Brazil. *Environ Pollut*. 2018;242:320–8. <https://doi.org/10.1016/j.envpol.2018.06.098>.
- Pearson C, Manning SW, Coleman M, Jarvis K. Can tree-ring chemistry reveal absolute dates for past volcanic eruptions? *J Archaeol Sci*. 2005;32:1265–74. <https://doi.org/10.1016/j.jas.2005.03.007>.
- Watmough SA. Monitoring historical changes in soil and atmospheric trace metal levels by dendrochemical analysis. *Environ Pollut*. 1999;106:391–403. [https://doi.org/10.1016/S0269-7491\(99\)0102-5](https://doi.org/10.1016/S0269-7491(99)0102-5).
- dos Santos SL, Viana LF, Mery FM, do Amaral Crispim B, Solorzano JC, Barufatti A, Cardoso CAL, Lima-Junior SE. Evaluation of the water quality in a conservation unit in Central-West Brazil: Metals concentrations and genotoxicity in situ. *Chemosphere*. 2020;251:126365. <https://doi.org/10.1016/j.chemosphere.2020.126365>.
- Seo E, Kim S, Park J, Lim H, Ha N, Lim J, Lim JH, Park HJ, Kim KH, Lee SJ. Foliar uptake of the potentially toxic elements in garlic chive leaves. *Front Environ Sci*. 2021;9:1–11. <https://doi.org/10.3389/fenvs.2021.702490>.
- Shaheen SM, Tsadilas CD, Rinklebe J. A review of the distribution coefficients of trace elements in soils: influence of sorption system, element characteristics, and soil colloidal properties. *Adv Colloid Interface Sci*. 2013;201–202:43–56. <https://doi.org/10.1016/j.cis.2013.10.005>.
- US-EPA. Basic Information about Lead Air Pollution. In: United States Environ. Prot. Agency. <https://www.epa.gov/lead-air-pollution/basic-information-about-lead-air-pollution>. Accessed 1 Jan 2023, 2022.
- Sternbeck J, Sjödin Å, Andréasson K. Metal emissions from road traffic and the influence of resuspension – Results from two tunnel studies. *Atmos Environ*. 2002;36:4735–44. [https://doi.org/10.1016/S1352-2310\(02\)00561-7](https://doi.org/10.1016/S1352-2310(02)00561-7).
- US-EPA. Locating and estimating air emissions from sources of cadmium and cadmium compounds. United States Environ Prot Agency 1993.
- US-EPA. Air pollution aspects of barium and its compounds. United States Environ Prot Agency 1969.
- Gundlach-Graham A, Burger M, Allner S, Schwarz G, Wang HAO, Gyr L, Grolimund D, Hattendorf B, Günther D. High-speed, high-resolution, multielemental laser ablation-inductively coupled plasma-time-of-flight mass spectrometry imaging: part I. Instrumentation and two-dimensional imaging of geological samples. *Anal Chem*. 2015;87:8250–8. <https://doi.org/10.1021/acs.analchem.5b01196>.
- Francischini DS, Arruda MAZ. When a picture is worth a thousand words: molecular and elemental imaging applied to environmental analysis – A review. *Microchem J*. 2021;169:106526. <https://doi.org/10.1016/j.microc.2021.106526>.
- Sussulini A, Becker JS, Becker JS. Laser ablation ICP-MS: application in biomedical research. *Mass Spectrom Rev*. 2017;36:47–57. <https://doi.org/10.1002/mas.21481>.
- Van Acker T, Buckle T, Van Malderen SJM, van Willigen DM, van Unen V, van Leeuwen FWB, Vanhaecke F. High-resolution imaging and single-cell analysis via laser ablation-inductively coupled plasma-mass spectrometry for the determination of membranous receptor expression levels in breast cancer cell lines using receptor-specific hybrid tracers. *Anal Chim Acta*. 2019;1074:43–53. <https://doi.org/10.1016/j.aca.2019.04.064>.
- Dumková J, Smutná T, Vrlíková L, Dočekal B, Kristeková D, Večeřa Z, Husáková Z, Jakešová V, Jedličková A, Mikuška P, Alexa L, Coufalík P, Tvrdoňová M, Křůmal K, Vaculovič T, Kanický V, Hampl A, Buchtová M. A clearance period after soluble lead nanoparticle inhalation did not ameliorate the negative

- effects on target tissues due to decreased immune response. *Int J Mol Sci.* 2020;21:1–27. <https://doi.org/10.3390/ijms21228738>.
17. Gundlach-Graham A, Garofalo PS, Schwarz G, Redi D, Günther D. High-resolution, quantitative element imaging of an upper crust, low-angle cataclasis (Zuccale Fault, Northern Apennines) by laser ablation ICP time-of-flight mass spectrometry. *Geostand Geoanalytical Res.* 2018;42:559–74. <https://doi.org/10.1111/ggr.12233>.
 18. Mokgalaka NS, Torresdesy JLG. Laser ablation inductively coupled plasma mass spectrometry: principles and applications. *Appl Spectrosc Rev.* 2006;41:131–50. <https://doi.org/10.1080/05704920500510703>.
 19. Koch J, Günther D. Laser ablation inductively coupled plasma mass spectrometry. *Encycl Spectrosc Spectrom* 2017;526–532. <https://doi.org/10.1016/B978-0-12-803224-4.00024-8>
 20. Limbeck A, Galler P, Bonta M, Bauer G, Nischkauer W, Vanhaecke F. Recent advances in quantitative LA-ICP-MS analysis: challenges and solutions in the life sciences and environmental chemistry. *Anal Bioanal Chem.* 2015;407:6593–617. <https://doi.org/10.1007/s00216-015-8858-0>.
 21. Costa VC, Babos DV, Castro JP, Andrade DF, Gamela RR, Machado RC, Sperança MA, Araújo AS, Garcia JA, Pereira-Filho ER. Calibration strategies applied to laser-induced breakdown spectroscopy: a critical review of advances and challenges. *J Braz Chem Soc.* 2020;31:2439–51. <https://doi.org/10.21577/0103-5053.20200175>.
 22. Pessôa GDS, Lopes CA, Madrid KC, Arruda MAZ. A quantitative approach for Cd, Cu, Fe and Mn through laser ablation imaging for evaluating the translocation and accumulation of metals in sun flower seeds. *Talanta.* 2017;167:317–24. <https://doi.org/10.1016/j.talanta.2017.02.029>.
 23. Chacón-Madrid K, Arruda MAZ. Internal standard evaluation for bioimaging soybean leaves through laser ablation inductively coupled plasma mass spectrometry: a plant nanotechnology approach. *J Anal At Spectrom.* 2018;33:1720–8. <https://doi.org/10.1039/c8ja00254a>.
 24. Papanlioti EM, Parviainen A, Alpiste MJR, Marchesi C, Garrido CJ. Quantification of potentially toxic elements in food material by laser ablation-inductively coupled plasma-mass spectrometry (LA-ICP-MS) via pressed pellets. *Food Chem.* 2019;274:726–32. <https://doi.org/10.1016/j.foodchem.2018.08.118>.
 25. dos Santos Moreau P, Arruda MAZ. Direct analysis of tree rings using laser ablation-ICP-MS and quantitative evaluation of Zn and Cu using filter paper as a solid support for calibration. *J Anal At Spectrom.* 2022;37:795–804. <https://doi.org/10.1039/d1ja00414j>.
 26. Hirata J, Takahashi K, Sahoo YV, Tanaka M. Laser ablation inductively coupled plasma mass spectrometry for quantitative imaging of elements in ferromanganese nodule. *Chem Geol.* 2016;427:65–72. <https://doi.org/10.1016/j.chemgeo.2016.02.017>.
 27. Jochum KP, Stoll B, Herwig K, Willbold M. Validation of LA-ICP-MS trace element analysis of geological glasses using a new solid-state 193 nm Nd:YAG laser and matrix-matched calibration. *J Anal At Spectrom.* 2007;22:112–21. <https://doi.org/10.1039/b609547j>.
 28. Santos MC, Wagner M, Wu B, Scheider J, Oehlmann J, Cadore S, Becker JS. Biomonitoring of metal contamination in a marine prosobranch snail (*Nassarius reticulatus*) by imaging laser ablation inductively coupled plasma mass spectrometry (LA-ICP-MS). *Talanta.* 2009;80:428–33. <https://doi.org/10.1016/j.talanta.2009.06.080>.
 29. Jochum KP, Scholz D, Stoll B, Weis U, Wilson SA, Yang Q, Schwab A, Börner N, Jacob DE, Andreae MO. Accurate trace element analysis of speleothems and biogenic calcium carbonates by LA-ICP-MS. *Chem Geol.* 2012;318–319:31–44. <https://doi.org/10.1016/j.chemgeo.2012.05.009>.
 30. Hare D, Austin C, Doble P, Arora M. Elemental bio-imaging of trace elements in teeth using laser ablation-inductively coupled plasma-mass spectrometry. *J Dent.* 2011;39:397–403. <https://doi.org/10.1016/j.jdent.2011.03.004>.
 31. Moradi AB, Swoboda S, Robinson B, Prohaska T, Kaestner A, Oswald SE, Wenzel WW, Schulin R. Mapping of nickel in root cross-sections of the hyperaccumulator plant *Berkheya coddii* using laser ablation ICP-MS. *Environ Exp Bot.* 2010;69:24–31. <https://doi.org/10.1016/j.envexpbot.2010.02.001>.
 32. Hare D, Austin C, Doble P. Quantification strategies for elemental imaging of biological samples using laser ablation-inductively coupled plasma-mass spectrometry. *Analyst.* 2012;137:1527–37. <https://doi.org/10.1039/c2an15792f>.
 33. Virgilio A, Silva ABS, Nogueira ARA, Nóbrega JA, Donati GL. Calculating limits of detection and defining working ranges for multi-signal calibration methods. *J Anal At Spectrom.* 2020;35:1614–20. <https://doi.org/10.1039/d0ja00212g>.
 34. IUPAC. Compendium of Chemical Terminology - Gold Book 2012.
 35. ICH (2005) Validation of Analytical Procedures : Text and Methodology Q2 (R1). *Int Conf Harmon* 1994;17. http://www.ich.org/fileadmin/Public_Web_Site/ICH_Products/Guidelines/Quality/Q2_R1/Step4/Q2_R1__Guideline.pdf
 36. da Silva Gomes M, Carvalho GGA, Santos D, Krug FJ. A novel strategy for preparing calibration standards for the analysis of plant materials by laser-induced breakdown spectroscopy: a case study with pellets of sugar cane leaves. *Spectrochim Acta Part B.* 2013;86:137–41. <https://doi.org/10.1016/j.sab.2013.03.009>.
 37. Amais RS, Moreau PS, Francischini DS, Magnusson R, Locosselli GM, Godoy-Veiga M, Ceccantini G, Ortega Rodriguez DR, Tomazello-Filho M, Arruda MAZ. Trace elements distribution in tropical tree rings through high-resolution imaging using LA-ICP-MS analysis. *J Trace Elem Med Biol.* 2021;68:126872. <https://doi.org/10.1016/j.jtemb.2021.126872>.
 38. Silvestre DM, de Oliveira Leme F, Nomura CS, do Nascimento AN. Direct analysis of barium, calcium, potassium, and manganese concentrations in tobacco by laser-induced breakdown spectroscopy. *Microchem J.* 2016;126:545–50. <https://doi.org/10.1016/j.microc.2016.01.015>.
 39. Sathre R. Life-Cycle Energy and Carbon Implications of Wood-Based Products and Construction. *Mid Sweden University Doctoral Thesis* 34;2007.
 40. Mata MERMC, Duarte MEM, Alsemo GCS, Rodrigues E, Guedes MA, Cavalcanti ASRRM, Oliveira CCA. Obtenção de graviola em pó pelo processo de liofilização. *Rev Bras Prod Agroindustriais.* 2005;7:165–72. <https://doi.org/10.15871/1517-8595/rbpa.v7n2p165-172>.
 41. Prosapio V, Lopez-Quiroga E. Freeze-drying technology in foods. *Foods.* 2020;9:3–5. <https://doi.org/10.3390/foods9070920>.
 42. González AG, Herrador MÁ. A practical guide to analytical method validation, including measurement uncertainty and accuracy profiles. *Trends Anal Chem.* 2007;26:227–38. <https://doi.org/10.1016/j.trac.2007.01.009>.
 43. Hattendorf B, Hartfelder U, Günther D. Skip the beat: minimizing aliasing error in LA-ICP-MS measurements. *Anal Bioanal Chem.* 2019;411:591–602. <https://doi.org/10.1007/s00216-018-1314-1>.
 44. Loni YH, David K, Larrue S, Grambow B, Corona C, Ribet S, Chardon P, Montavon G. Uranium quantification of oak tree rings (*Quercus petraea*) from a former uranium mining site by High Resolution Inductively Coupled Plasma Mass spectrometry in Laser Ablation and Solution modes. *Spectrochim Acta*

- Part B At Spectrosc. 2019;161:105709. <https://doi.org/10.1016/j.sab.2019.105709>.

Publisher's Note Springer Nature remains neutral with regard to jurisdictional claims in published maps and institutional affiliations.

Springer Nature or its licensor (e.g. a society or other partner) holds exclusive rights to this article under a publishing agreement with the author(s) or other rightsholder(s); author self-archiving of the accepted manuscript version of this article is solely governed by the terms of such publishing agreement and applicable law.